

The Toarcian Oceanic Anoxic Event in the Ionian Zone, Greece

N. Kafousia ^{a,*}, V. Karakitsios ^a, E. Mattioli ^b, S. Kenjo ^b, H.C. Jenkyns ^c

^a Department of Historical Geology and Paleontology, Faculty of Geology and Geoenvironment, National and Kapodistrian University of Athens, Panepistimiopolis, 15784 Athens, Greece

^b Laboratoire de Géologie de Lyon UMR 5276 CNRS, Université Lyon 1, ENS Lyon, Campus de la Doua, Bâtiment Géode, F-69622 Villeurbanne Cedex, France

^c Department of Earth Sciences, University of Oxford, South Parks Road, Oxford OX1 3AN, United Kingdom



ARTICLE INFO

Article history:

Received 4 April 2013

Received in revised form 12 November 2013

Accepted 14 November 2013

Available online 25 November 2013

Keywords:

Jurassic

Carbon isotopes

Chemostratigraphy

Calcareous nannofossils

T-OAE

ABSTRACT

The Early Jurassic was characterized by a global disturbance of the carbon cycle known as the Toarcian Oceanic Anoxic Event (T-OAE). This event is recorded worldwide by a negative excursion in marine and terrestrial carbon-isotope ratios, typically interrupting an overarching positive trend attributed to large-scale burial of marine organic matter under oxygen-depleted conditions. The negative excursion is attributed to introduction of isotopically light carbon into the ocean-atmosphere system. Three sections from the Ionian Zone in Greece have been analysed in terms of biostratigraphy, Total Organic Carbon (TOC), CaCO_3 , $\delta^{13}\text{C}_{\text{carb}}$, $\delta^{18}\text{O}_{\text{carb}}$ and $\delta^{13}\text{C}_{\text{org}}$. On the basis of bio- and chemostratigraphy, the age of Pliensbachian-Toarcian formations from the Ionian Zone in Greece has been refined and the geochemical signature of the T-OAE recognized. All sections illustrate the characteristic negative excursion in carbon isotopes from both carbonates and organic matter and, in only one locality, a positive excursion has also been recorded. The recognition of the T-OAE in this part of the Tethyan continental margin offers additional information on the global impact and amplitude of this important Jurassic palaeoceanographic event.

© 2013 Published by Elsevier B.V.

1. Introduction

The Toarcian Oceanic Anoxic Event (T-OAE) constitutes one of the most dramatic climatic events of the Mesozoic Era (Jenkyns, 1988), and caused perturbation in the global carbon (Hesselbo et al., 2000) and sulphur cycles (Gill et al., 2011; Newton et al., 2011). The event is marked by enhanced marine carbon burial (Jenkyns, 1985, 1988, 2010; Sabatino et al., 2009; Kafousia et al., 2011) and coincides with a negative excursion in carbon isotopes interrupting an overarching positive trend. The carbon-isotope excursion (CIE) has been recorded in different materials, such as terrestrial wood (Hesselbo et al., 2000; Hesselbo et al., 2007; Al-Suwaidi et al., 2010), marine organic matter, pelagic and shallow-water carbonate (Jenkyns and Clayton, 1986; van Breugel et al., 2006; Suan et al., 2008; Woodfine et al., 2008; Sabatino et al., 2013). The isotopic response was registered in the European epicontinental seaway (Sælen et al., 1996; Jenkyns and Clayton, 1997; van de Schootbrugge et al., 2005a), southern Tethyan margin exposed in central Italy (Jenkyns and Clayton, 1986; Mattioli et al., 2004; Sabatino et al., 2011), North Africa (Bodin et al., 2010); Pindos Zone of Greece (Karakitsios et al., 2010; Kafousia et al., 2011), Palaeo-Pacific/Japan (Gröcke et al., 2011), Neuquén Basin, Argentina (Al-Suwaidi et al., 2010; Mazzini et al., 2010), Canada (Caruthers et al., 2011), and Siberia (Suan et al., 2011; Fig. 1A & B).

This oceanic anoxic event was associated with global warming (Bailey et al., 2003; Jenkyns, 2003; Suan et al., 2008), mass extinction

(Little and Benton, 1995; Wignall, 2001) and probable ocean acidification (Hermoso et al., 2012; Hönsch et al., 2012; Trecall et al., 2012). The causes for this event are still under debate, with most plausible explanations related to introductions of high nutrient loads into the oceans under conditions of an accelerated hydrological cycle stimulating plankton productivity and carbon flux to the sea floor (Jenkyns, 2010). A phenomenon accompanying the increase in organic-matter deposition was introduction of isotopically light carbon into the ocean-atmosphere system from the dissociation of methane hydrates and/or hydrothermal venting of greenhouse gases (Hesselbo et al., 2000; Svensen et al., 2007).

The Toarcian sediments that have already been studied in detail from Greece belong to the Pindos Zone (Kafousia et al., 2011): a deep-sea ocean-margin basin that formed in mid-Triassic times along the northeastern part of Apulia. In this paper, we present biostratigraphical (calcareous nannofossils) and geochemical (wt.% TOC, wt.% CaCO_3 , $\delta^{13}\text{C}_{\text{carb}}$, $\delta^{18}\text{O}_{\text{carb}}$ and $\delta^{13}\text{C}_{\text{org}}$) data from three sections from the Ionian Zone, a marine basin that constituted part of the southern Tethyan margin (Bernoulli and Renz, 1970). All three sections belong to the same palaeogeographic zone but present several differences, mainly because they belong to different sub-basins, each of which had its particular palaeogeographic characteristics.

2. Geological setting and stratigraphy

The Ionian Zone of northwestern Greece (Epirus region) constitutes part of the most external Hellenides (Paxos Zone, Ionian Zone, Gavrovo Zone; Fig. 1C). These zones correspond to the Hellenic domain of the

* Corresponding author. Tel.: +30 2107274370.

E-mail address: nkafousia@geol.uoa.gr (N. Kafousia).

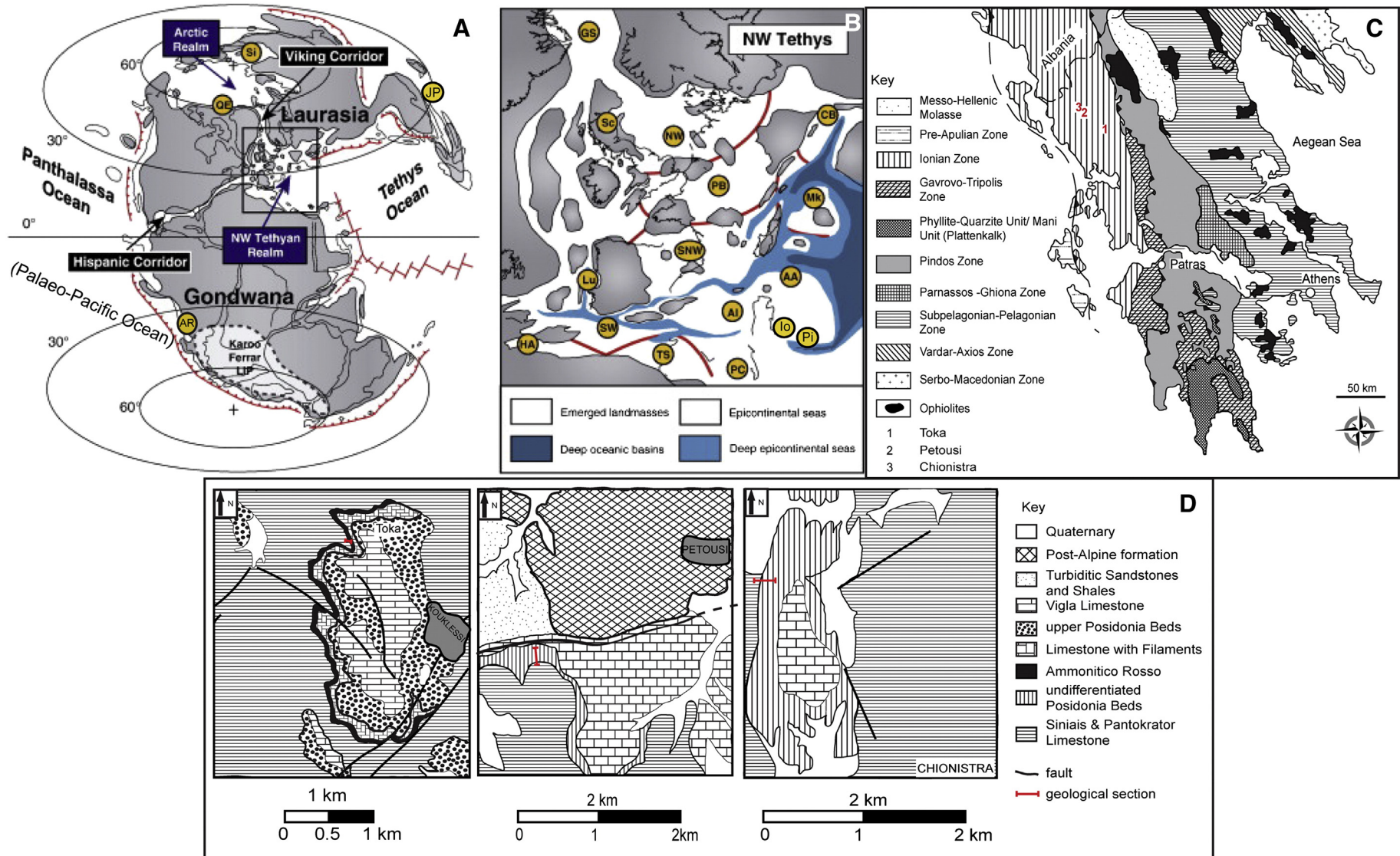


Fig. 1. A & B: Palaeogeographic map of Pliensbachian–Toarcian boundary (modified from Dera et al., 2011). Si: Siberia, JP: Japan, QE: Queen Elizabeth Islands, Canada, GS: Greenland–Spitsbergen, Sc: Scotland, NW: NW Europe, CB: Carpathian–Balkan areas, PB: Paris Basin, Mk: Meksek, Hungary, SNW: North of NW Europe, Lu: Lusitanian Basin, AA: Austro- and southern Alpine regions, Al: Apennines, Ionian islands, PC: Peloritanian–Calabrian regions, TS: Tunisia, Sicily, SW: SW Tethys, HA: High Atlas, Morocco, Io: Ionian Zone, Greece, Pi: Pindos Zone, Greece. C: simplified geological map of Greece. D: geological map of the studied sections.

southern passive continental margin associated with Early Mesozoic opening and late Mesozoic–Early Cenozoic closure of the Neotethys Ocean (Laubscher and Bernoulli, 1977; Karakitsios, 1992, 1995). The rocks represented in the Ionian Zone range from Triassic evaporites through a varied series of Jurassic to Upper Eocene mixed carbonate–siliciclastic–siliceous sediments, overlain by Oligocene turbidites and shales (locally termed “flysch”). In the Early Jurassic, northwestern Greece was covered by a vast carbonate platform (Bernoulli and Renz, 1970; Walzebuck, 1982; Karakitsios, 1992, 1995). In the Pliensbachian, the area of study was affected by extensional tectonics related to the opening of the Neotethys Ocean (Karakitsios, 1995). These stresses caused the differentiation of the Ionian Zone from the adjacent Paxos and Gavrovo Zones (Karakitsios, 1992, 1995). While the latter Zones remained as carbonate platforms, the Ionian basin became an area of strong subsidence and faulting with the development of pelagic conditions (Karakitsios, 1995). This palaeogeographic evolution is recorded in the pelagic Siniás Limestone and the laterally equivalent Louros Limestone of Pliensbachian Stage (Bernoulli and Renz, 1970; Walzebuck, 1982; Karakitsios and Tsaila-Monopolis, 1988; Karakitsios, 1992; Dommergues et al., 2002).

The initial formation of the Ionian basin was followed by an internal differentiation into smaller palaeogeographic sub-basins (Walzebuck, 1982; Baudin et al., 1990; Karakitsios, 1995;) with half-graben geometry, generally not exceeding 5 km in width (Karakitsios, 1995). This complex palaeogeography resulted in abrupt changes in thickness of the syn-rift formations, which take the shape of syn-sedimentary wedges (Karakitsios, 1992, 1995). In the deeper parts of the half-grabens, these include complete Toarcian–Tithonian successions comprising from base to top: lower Posidonia Beds or Ammonitico Rosso of Toarcian–Aalenian Stage (Aubouin, 1959; IGRS-IFP, 1966; Baudin et al., 1990; Karakitsios, 1992), Limestone with Filaments of Bajocian–Callovian Stage (Karakitsios et al., 1988) and the upper Posidonia Beds of Callovian–Tithonian Stage (Karakitsios et al., 1988). In the shallower parts of the half-grabens, the succession is interrupted by hiatuses and unconformities. The directions of syn-sedimentary structures (e.g. slumps and syn-sedimentary faults) indicate that deposition was controlled both by structures formed during extension related to the opening of the Neotethys Ocean and the halokinesis of evaporites at the base of the Ionian Zone succession (Karakitsios, 1992, 1995). This particular geometry of the restricted sub-basins that were formed during the syn-rift period of the Ionian Zone may have favoured increased organic-matter burial during the Toarcian–Tithonian interval (Karakitsios, 1995; Rigakis and Karakitsios, 1998; Karakitsios and Rigakis, 2007). Toarcian black shales in the Ionian Zone were described first by Renz (1910), who compared them with the Posidonienschifer of Germany, and sedimentological details were given by Walzebuck (1982). In this paper we demonstrate that these Lower Toarcian organic-rich laminated black shales deposited in different palaeogeographic environments are represented in all the Ionian sub-basins and record a global rather than a local event.

2.1. Toka section

The Toka section ($39^{\circ}23'N$, $20^{\circ}50'E$), described by Karakitsios (1992), is located W-NW of Ano Kouklessi village in the prefecture of Ioannina. The outcrop is of excellent quality and shows, in stratigraphic continuity, the Siniás Limestone, Toka Shales and marly Ammonitico Rosso (Fig. 1D). The sampled section begins in the uppermost metres of Siniás Limestone, comprising grey limestones with intercalations of green-grey marls. The section continues with 11 m of blue laminated marls, intercalated between black shales and marly limestones (Toka Shales), 9 m of marly Ammonitico Rosso (red marls alternating with greenish marly limestones) and ends in the first few metres of nodular Ammonitico Rosso (nodular limestones with green nodules, red marly matrix and intercalations of thin red marls).

2.2. Petousi section

The Petousi section ($39^{\circ}30'N$, $20^{\circ}35'E$), also described by Karakitsios (1992), is located around 2 km WSW from Petousi village, south of the Petousi–Paramythia road, in Thesprotia prefecture. The studied outcrop is also of excellent quality even though it is locally covered by vegetation. The section (Fig. 1D) begins with the uppermost metres of the Siniás Limestone (white to grey limestones, with thin layers of black shales intercalated in its upper part). The outcrop continues with undifferentiated Posidonia Beds, which begins with 10 m of black shales followed by a yellow-green chert rich in *Posidonia* (*Bositra buchi*).

2.3. Chionistra section

The geology of the area was first described by Walzebuck (1982). The specific section of Chionistra ($39^{\circ}32'N$, $20^{\circ}30'E$), has been described by Karakitsios (1992). It is located around 1 km SW of Elataria village in Thesprotia prefecture. The outcrop (Fig. 1D) begins in the uppermost metre of the Siniás Limestone (well-bedded limestones with nodular intercalations) and continues with 17 m of lower Posidonia Beds. In the lower part of this formation fossil remains of the conifer *Brachyphyllum nepos* SAPORTA has been found that indicates a tropical environment (Karakitsios, 1992, 1995; Karakitsios and Velitzelos, 1994). This section was sampled at relatively low resolution with a total of 33 samples.

3. Methodology

A total of 227 samples (55 from Toka, 139 from Petousi, 33 from Chionistra) were analysed for their wt.% TOC and wt.% CaCO_3 contents using a Strohlein Coulomat 702 analyser (details in Jenkyns, 1988). For carbonate carbon- and oxygen-isotope composition, 401 bulk sediment samples (157 Toka, 211 Petousi, 33 Chionistra) were powdered and analysed using a VG Isogas Prism II mass spectrometer (details in Jenkyns et al., 1994). For 386 samples (142 Toka, 97 Petousi, 33 Chionistra) organic carbon-isotope composition was measured using a Europa Scientific Limited CN biological sample converter connected to a 20–20 stable-isotope gas-ratio mass spectrometer (details in Jenkyns et al., 2007). The above analyses were undertaken in the Department of Earth Sciences and Research Laboratory for Archaeology in the University of Oxford.

A set of 85 samples was investigated for the content of calcareous nannofossils. Smear-slides were prepared from the powdered rock according to the technique described in Bown and Young (1998), then analysed in an optical polarizing Leitz microscope at $\times 1250$. Nannofossils were counted for each sample in a surface area of the slide varying between 0.2 and 0.3 cm^2 at the Laboratoire de Géologie de Lyon, Université Lyon 1.

4. Results

4.1. Biostratigraphy

4.1.1. Toka section

Twenty-eight samples from the Toka section were studied for their calcareous nannofossil content, as represented in Fig. 2. All the analysed samples were relatively poor in nannofossils, and overall preservation was poor. In spite of the limited preservation, species richness was moderate to relatively high, especially in the Toka Shales. In general, assemblage composition resembles what is recorded in Central Italy; hence the zonal scheme of Mattioli and Erba (1999) was used for this work. The base of the section (Siniás Limestone) was not analysed for nannofossil content. The NJT 6 Zone was clearly identified based on the presence of *Carinolithus superbus* from the base of the analysed interval (basal part of the Toka Shales). The first occurrence (FO) of *Discorhabdus striatus*, followed by the last occurrence (LO) of

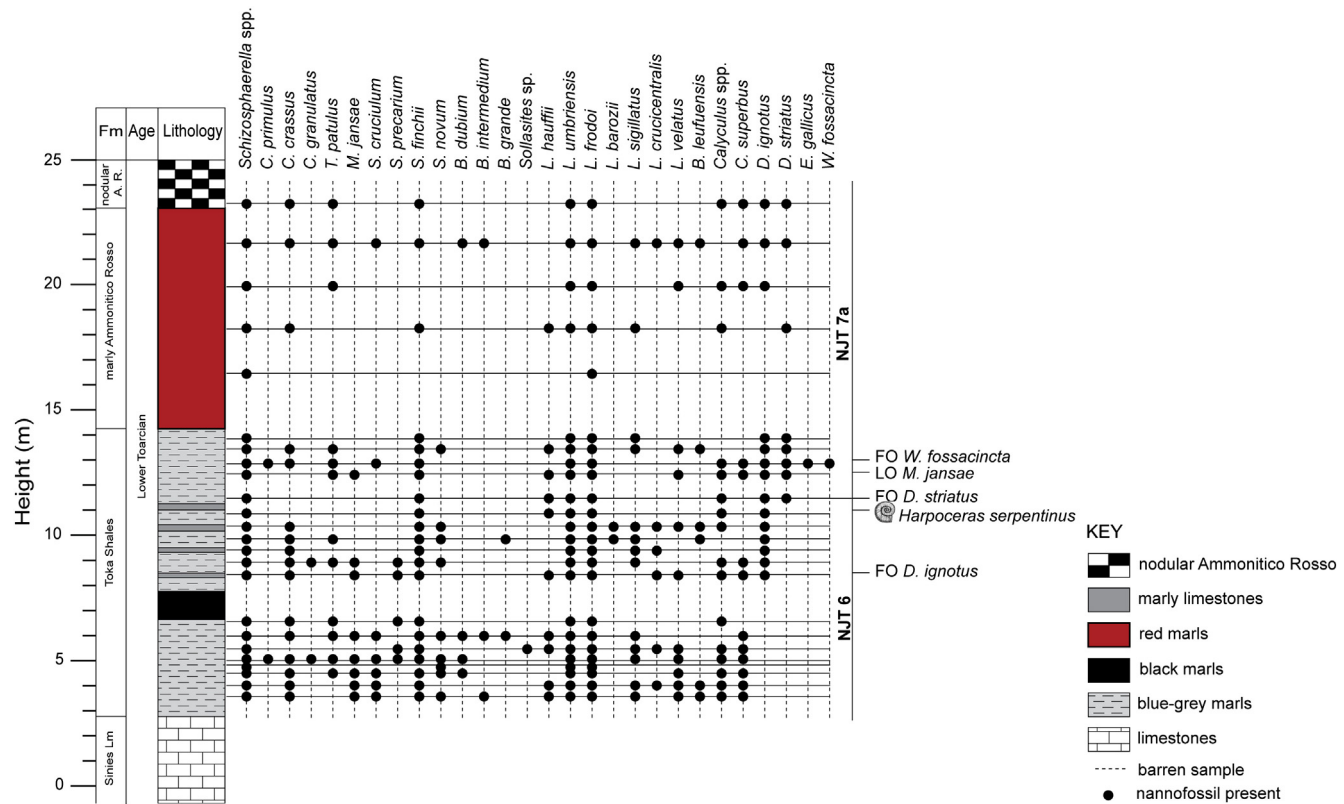


Fig. 2. Calcareous nannofossil biostratigraphy of the Toka section. Because of the relatively poor nannofossil record, only the presence (black dot) or absence of various taxa is shown.

Mitrolithus jansae and by the FO of *Watznaueria fossacincta* was used to identify the subsequent NJT 7 Nannofossil Zone starting at 11.60 m.

In addition, in sample TOK-80 (at 11 m in the section) an imprint of an ammonite was found. This ammonite was identified by Dr Lutomir Metodiev (Bulgarian Academy of Science) as *Harpoceras serpentinum* (Schlotheim, 1983), belonging to the ammonite subzone *H. serpentinum*, which corresponds to the lower part of the ammonite Zone *Harpoceras falciferum* (Metodiev, 2008). This ammonite is recorded within the upper part of the Nannofossil Zone NJT 6 recognized in the present work (s. supra). This integrated biostratigraphic record is consistent with what has been reported from Central Italy (Mattioli and Erba, 1999).

4.1.2. Petousi section

Twenty-four samples from the Petousi section were studied, which show a diverse and relatively rich nannofossil assemblage, although preservation is moderate to poor (Fig. 3). *Schizosphaerella*, *Mitrolithus jansae* and some small *Lotharingius* (namely, *Lotharingius hauffii* and *Lotharingius frodoi*) are the dominant forms in the assemblage. The base of the section, corresponding to the Siniens Limestone, is dated as NJT 5b, because of the presence of *Calyculus* spp. and *Lotharingius sigillatus*. This Zone spans the Pliensbachian–Toarcian boundary. At 5.4 m, the FO of *Carinolithus superbus* is observed, testifying to the presence of the NJT 6 Zone, which finishes at 9.8 m with the FO of *Discorhabdus striatus* that marks the onset of the NJT 7 Zone.

4.1.3. Chionistra section

The thirty-three samples analysed from the Chionistra section are relatively poor in terms of nannofossil abundance and preservation, although all samples contain calcareous nannofossils, as can be seen in Fig. 4. Typical Tethyan taxa, such as *Mitrolithus jansae*, dominate the assemblage. The presence of *Carinolithus poulnabronei* and *Carinolithus superbus* allows us to recognize the NJT 6 Zone, but its

lower and upper boundary remain uncertain because no biostratigraphic event (first or last occurrence) could be identified in under- or overlying strata.

4.2. wt.% Total Organic Carbon (TOC) and wt.% CaCO₃

4.2.1. Toka section

The results for TOC and CaCO₃ for the Toka section are represented in Fig. 5. The TOC values are very low in the few samples analysed in the lower part of the section. In the basal Toka Shales, TOC values begin to rise, marking a positive excursion that reaches values up to 2.41 wt%. At the top of this excursion, values return to background and rise up again for the main positive excursion where values up to 5.15 wt% are measured. After this maximum value, that is located in the 7-metre level of the section, values drop sharply close to zero. For the next 3 m, TOC values fluctuate between 0 and 1%. After that and until the end of the section values are again close to zero.

The carbonate values are in general relatively high, with a mean value of 41.99 wt%. The percentage drops to very low values (3.98 wt%) in the black shales, but after the 8-metre level of the section, values rise again. Above the 12-metre level, CaCO₃ values fluctuate above 60 wt%.

4.2.2. Petousi section

TOC values in this section begin at very low values (~0–1 wt%), in the Siniens Limestone (Fig. 6). Values begin to rise in the basal levels of the undifferentiated Posidonia Beds where there are black shales, with TOC values rising to 4.86 wt% over a 2-metre interval and defining a positive excursion. After this peak, values are lower, although background values are not attained, fluctuating between ~0 and 3 wt%. CaCO₃ values are in general high with very few exceptions. In the interval of the positive TOC excursion, CaCO₃ values are low, as also recorded in the Toka section, and fall to 2.64 wt%. Higher in the section, values increase and fluctuate around a mean of 55 wt%.

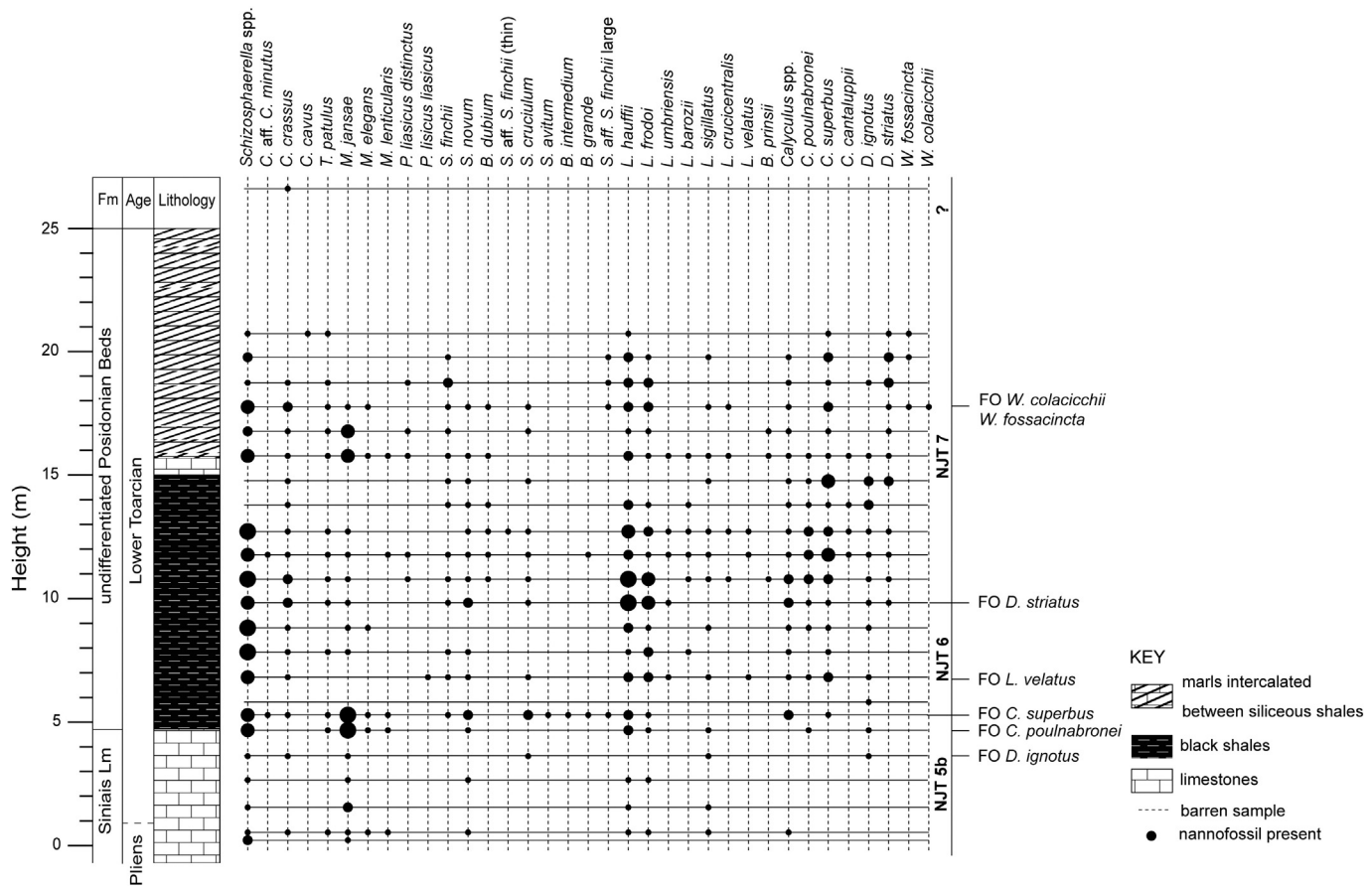


Fig. 3. Biostratigraphy of the Petousi section. Because calcareous nannofossil content is richer than in the two other sections, relative abundance per square surface unit was estimated. Four abundance classes were defined: rare, frequent, common and abundant. These classes are represented by different sizes of black dots.

4.2.3. Chionistra section

TOC in the Chionistra section begins with very low values, ~0.1 wt.%, and rises up to the 7-metre level of the section with no particular trend or fluctuations between 0.1 and 1.6 wt.% (Fig. 7). CaCO₃ values are in general high, with mean values of 58.4 wt.%. In the lower part of the section values are close to 70 wt.%, and remain high up to the 7-metre level. Up-section they show considerable variability, in general, staying high, with a few exceptions as low as 20 wt.%.

4.3. Stable-isotope ratios

4.3.1. Toka section

The overall trends in δ¹³C_{carb} and δ¹³C_{org} at Toka are broadly similar (Fig. 5), though the organic carbon-isotope data show a higher degree of scatter. Bulk-rock δ¹³C_{carb} values are about 3‰ at the base of Siniais Limestone. The values are stable up to the top of this formation, except for a minor positive excursion of ~1‰. Passing to the Toka Shales, the isotopic values drop to 0.5‰, then return to 2‰ and drop again to 0‰. This negative excursion ends at the 10-metre level of the section. A small positive excursion, which reaches values up to 4.5‰, follows the negative excursion. δ¹³C_{carb} values reach background values of 3.5‰ at the 15-metre level.

In the Siniais Limestone, organic carbon-isotope values are stable at background levels of ~−26‰. In the basal Toka Shales, values fall and define the negative excursion that spans the interval from the 3- to 8-metre level of the section where values drop to −32‰. Above the 8-metre level in the section, values rise gradually till the top of this formation at the 14-metre level. Up-section, values fluctuate around background values of ~−26‰.

The δ¹⁸O_{carb} profile begins with low values of −2.5‰ in the Siniais Limestone. In the Toka Shales, values rise and fluctuate over 6 metres of section. Stratigraphically higher in the section, nearly at the end of the negative carbon-isotope excursion, δ¹⁸O_{carb} records a negative excursion that lasts for 1 m. This negative shift is followed by a return to higher δ¹⁸O_{carb} values. Higher in the section, values are stable and fluctuate around 1.7‰.

4.3.2. Petousi section

Both carbonate and organic-carbon δ¹³C profiles show a small disturbance at the 2-metre level of the section, as it can be seen in Fig. 6. This, together with the small increase in the TOC profile and the biostratigraphic data, indicates that this is the Pliensbachian-Toarcian boundary. Above this boundary, isotopic values of bulk carbonate remain stable around 1.3‰. The values show a marked ~1‰ decrease half a metre above the NJT 5b/NJT 6 boundary. The negative excursion spans less than 1 m. Values increase above this level. The positive excursion that follows may be of only ~1‰, but spans 11 metres. Higher in the section, values decrease again.

Organic carbon-isotope data differ in some degree from carbonate isotopic data in terms of their general profiles. Above the perturbation in the lower part of the section, δ¹³C_{org} fluctuates around a background value of −29‰. At the NJT 5b/NJT 6 boundary, values record the characteristic negative excursion. Values fall by ~4‰ to ~−33‰. This excursion spans 2 m of section. Up-section, values return to background levels rising again to −30‰. Above this point, δ¹³C_{org} fluctuates between the 7 m and 9.5-metre level of the section where a positive shift is recorded with values rising to ~−26‰. The positive excursion also spans 2 metres of section. Above this level, values return to background levels of ~−29‰.

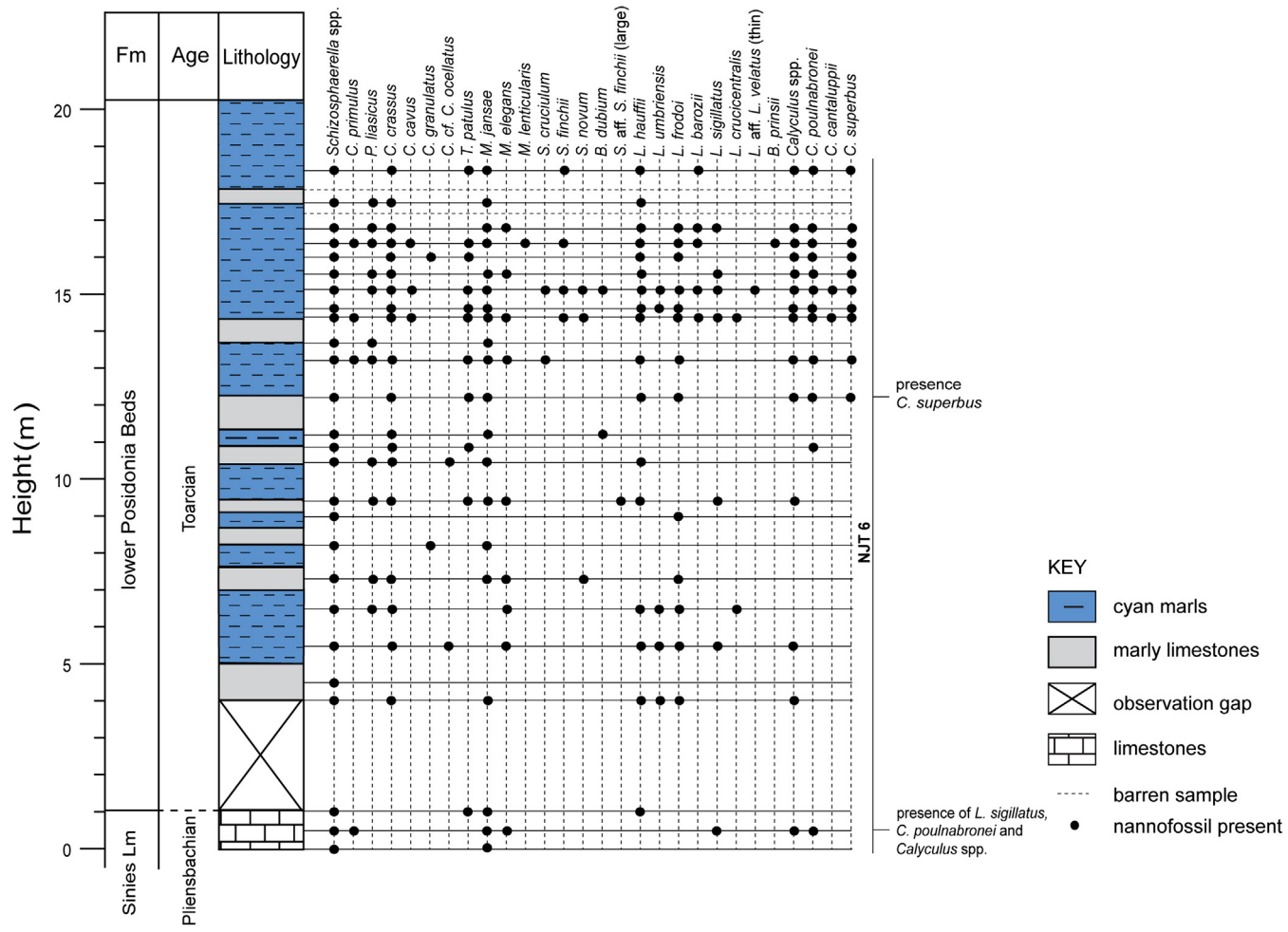


Fig. 4. Calcareous nannofossil biostratigraphy of the Chionistra section. The upper and lower boundaries of the NJT 6 Nannofossil Zone are uncertain.

Oxygen-isotope values are more or less stable throughout the entire section. Looking in detail, there are strong fluctuations up to the Pliensbachian–Toarcian boundary. Higher in the section, values remain stable until approximately the level of the major negative carbon-isotope excursion, where $\delta^{18}\text{O}_{\text{carb}}$ reaches values as low as $-4\text{\textperthousand}$. After that level, values are unstable and fluctuate between -5 and $-2.5\text{\textperthousand}$ until the 9-metre level of the section. From the 9-metre, and just below the 20-metre level of the section, values are relatively stable at $-2.5\text{\textperthousand}$. Above this level, and up to the top of the section, values decline to a minimum value of $-7.72\text{\textperthousand}$.

4.3.3. Chionistra section

Despite being sampled at relatively low resolution, general chemostratigraphic trends can be discerned in this section (Fig. 7). Carbonate carbon-isotope values at the base of the section are around $1.8\text{\textperthousand}$ and are followed by a negative excursion, spanning 8 m of section, with values falling to $0.93\text{\textperthousand}$. Following this excursion, values begin to rise. From the 10.5- to the 16.5-metre level of the section, values record a positive excursion with maximum value of $2.39\text{\textperthousand}$. Above this level, $\delta^{13}\text{C}_{\text{carb}}$ attains background values ($\sim 1.8\text{\textperthousand}$) to the top of the section.

Organic carbon-isotope data record a small negative excursion in the first metre of the section; the minimum value attained is $-33.14\text{\textperthousand}$. Higher in the section, values increase and then decrease again. This second negative excursion displays values down to $-31\text{\textperthousand}$ up to the 8-metre level of the section. Above this, values fluctuate around $-27\text{\textperthousand}$, continuing to the top of the section.

Oxygen-isotope values do not follow any particular trend and fluctuate between -2.57 to $-1.82\text{\textperthousand}$ throughout the entire section.

5. Discussion

5.1. Biostratigraphy and chemostratigraphy

Examination of nannofossils from the Ionian Zone gives direct and detailed biostratigraphic control for these formations. Here we confirm the Toarcian Stage of the marls at the base of Ammonito Rosso (Toka Shales), the lower Posidonia Beds and the lower part of the undifferentiated Posidonia Beds.

The upper part of the Sinias Limestone belongs to Subzone NJT 5b *Lotharingius sigillatus*, spanning the Upper Pliensbachian–Lower Toarcian interval (Mattioli and Erba, 1999; Mattioli et al., 2009), as can be seen from the Petousi biostratigraphic data. In the same section there is also a small negative followed by a small positive excursion in carbonate carbon-isotopic data. The combination of these two stratigraphic indices indicates that the Pliensbachian–Toarcian boundary is recorded in the uppermost metres of the Sinias Limestone of the Petousi section. Because a similar event has been recognized in other European sections, the small negative carbon-isotope excursion likely represents an event of global significance: in many areas the amplitude of the Pliensbachian–Toarcian boundary negative excursion is equal to that of the main excursion in the Early Toarcian (Hesselbo et al., 2007; Sabatino et al., 2009; Bodin et al., 2010; Littler et al., 2010; Kafousia et al., 2011). A small hiatus or level of stratigraphic condensation in the other sections from the Ionian Zone is not excluded at the Pliensbachian–Toarcian boundary, as already observed in several western Tethys sections (central Italy, Mattioli et al., 2004; NE France, van Breugel et al., 2006; S France,

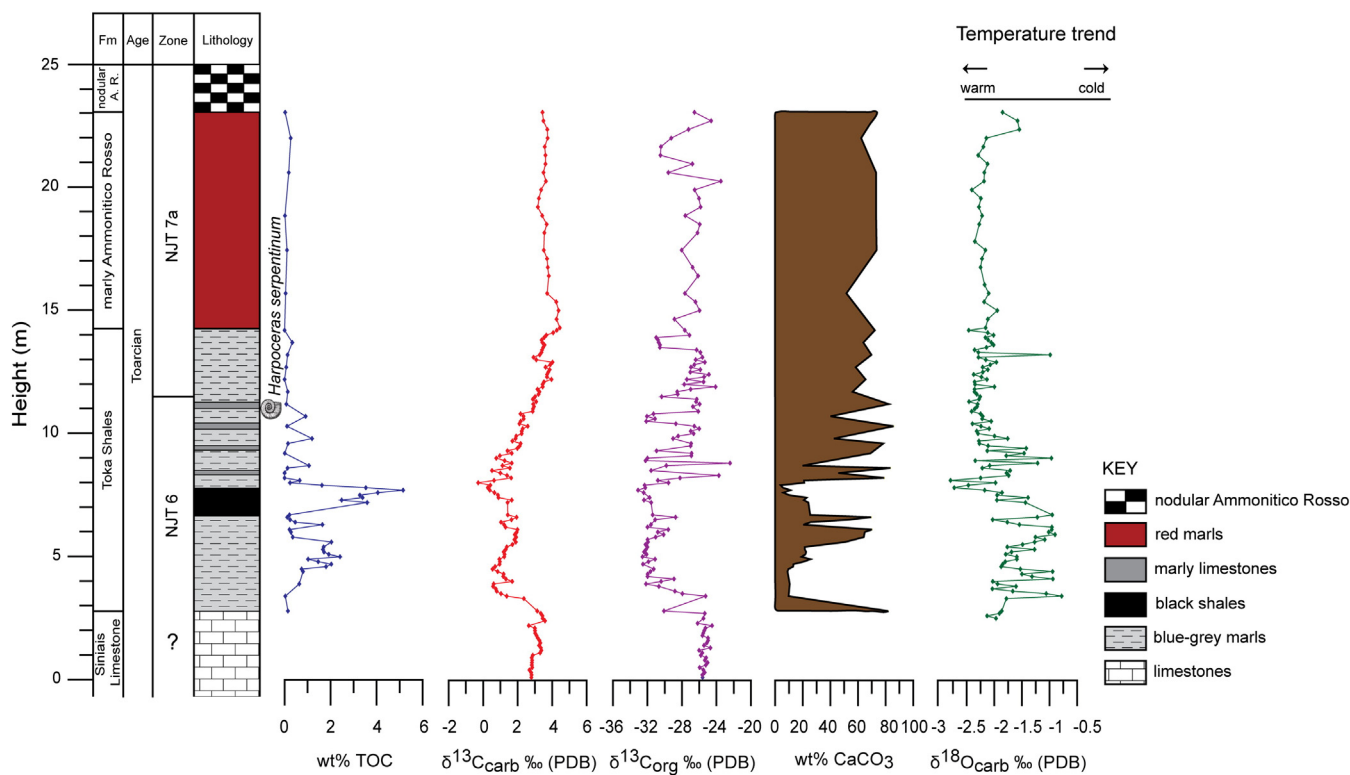


Fig. 5. Lithostratigraphic log, bulk TOC, $\delta^{13}\text{C}_{\text{carb}}$, $\delta^{13}\text{C}_{\text{org}}$ wt.% CaCO₃ and $\delta^{18}\text{O}_{\text{carb}}$ profiles through the Toka section (analytical data in S1).

Mailliot et al., 2009; SE France, Léonide et al., 2012; Portugal, Suan et al., 2010).

The lower part of the overlying formation (Toka Shales, undifferentiated Posidonia Beds or lower Posidonia Beds) belongs to the Nannofossil Zone NJT 6 *Carinolithus superbus*. This Zone is encapsulated in the ammonite Zones *polymorphum/tenuicostatum* and *levisoni/*

serpentinus in Tethyan sections where ammonite biostratigraphy is available (Mattioli and Erba, 1999; Mattioli et al., 2009). This stratigraphic assignment is further confirmed by the presence of the ammonite *Harpoceras serpentinus* in the sample TOK-80.

When correlating biostratigraphy and chemostratigraphy between the three sections from the Ionian Zone, it appears that the

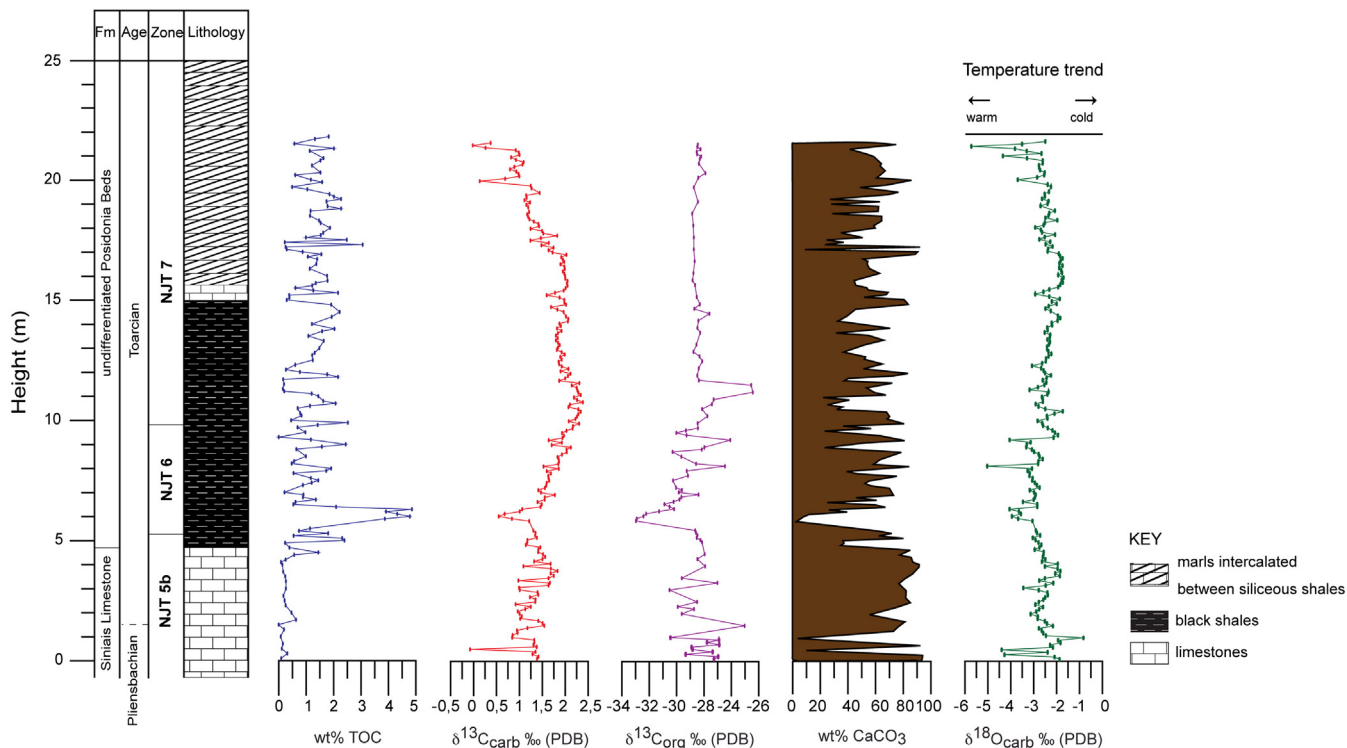


Fig. 6. Lithostratigraphic log, bulk TOC, $\delta^{13}\text{C}_{\text{carb}}$, $\delta^{13}\text{C}_{\text{org}}$ wt.% CaCO₃ and $\delta^{18}\text{O}_{\text{carb}}$ profiles through the Petousi section (analytical data in S2).

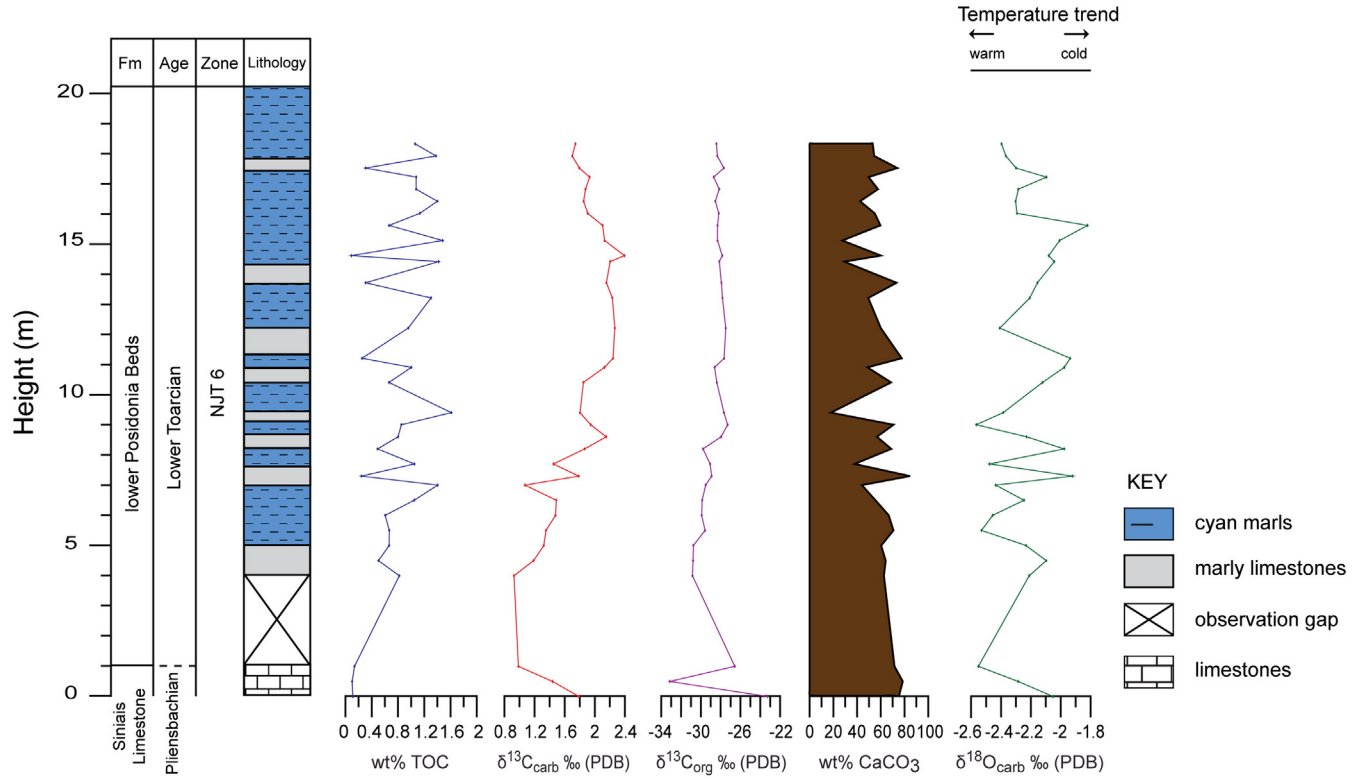


Fig. 7. Lithostratigraphic log, bulk TOC, $\delta^{13}\text{C}_{\text{carb}}$, $\delta^{13}\text{C}_{\text{org}}$, wt.% CaCO_3 and $\delta^{18}\text{O}_{\text{carb}}$ profiles through the Chionistra section (analytical data in S3).

main negative carbon-isotope excursion and the TOC enrichment correspond to the NJT 6 Zone, as already shown for many sections in western Tethys (Mattioli et al., 2009). In the higher levels of the sections, the facies differ. In the Toka section, the Toka Shales pass upward to the marly Ammonitico Rosso that corresponds to the NJT 7a Subzone *Discorhabdus striatus*, spanning the interval from the upper part of the Lower Toarcian to the top of the Middle Toarcian (Mattioli and Erba, 1999). In the Petousi section, the base of the NJT 7a Subzone occurs within the organic-rich black shales. Chionistra is more difficult to interpret in terms of biostratigraphy, but it seems that the NJT 6 Zone spans the whole section, although the exact positions of the base and the top of the Zone are uncertain.

5.2. Organic matter content

Total organic-carbon values in the Ionian Zone are comparable with coeval Tethyan sections. In the Toka and Petousi sections, TOC values over the interval of the negative carbon-isotope excursion reach values up to ~5%. These values are similar to those in certain pelagic sections from the Southern Alps of Italy (Jenkyns et al., 2001; Pancost et al., 2004; Jenkyns, 2010). Conversely, TOC values from Chionistra are lower, only attaining ~2%. These values are similar to those recorded from the central Apennines of Italy and some other sections in the Southern Alps (Bellanca et al., 1999; Mattioli et al., 2004; Sabatino et al., 2011).

A difference is observed between the Toka and Petousi sections; in the former TOC values are high only in the interval corresponding to the negative carbon-isotope excursion whereas, in the latter, values approach 0% in the interval preceding the CIE, and at higher levels fluctuate between 0 and 2%. This difference must indicate some degree of local control on palaeoenvironmental conditions.

5.3. Recognition of the Toarcian Oceanic Anoxic Event in the Ionian Zone

Toarcian organic-rich shales in the Ionian and Pindos Zones of Greece were attributed to the Toarcian Oceanic Anoxic Event (T-OAE)

by Jenkyns (1988), based on general stratigraphic considerations. The chemo- and biostratigraphic data presented here indicate that this interpretation was correct. The biostratigraphic data place the described sections between the Upper Pliensbachian and the Lower Toarcian Stages and the geochemical data confirm the exact level of the Pliensbachian–Toarcian boundary and the Toarcian Oceanic Anoxic Event, particularly in the two sections sampled at high resolution. In all sections the NJT 6 Zone coincides with a negative excursion in the carbon-isotope record as well as with a positive excursion in TOC that is the defining characteristic of the T-OAE.

5.4. Carbon-isotope trends and timing

One of the most significant features of the T-OAE in the Ionian Zone is the perturbation of the carbon-isotope trend. The carbon-isotope excursions of the two high-resolution sections (Toka and Petousi) reveal differing trends. The pattern is different not only between the sections but also between the carbonate and organic carbon-isotopes. The organic matter has an isotopic composition slightly different in the two sections, although the analysis of the OM is beyond the scope of this paper. The negative CIE in the Toka section in both carbon-isotopes spans an interval of ~6 m. The negative excursion in the carbonate carbon-isotope record is followed by a small positive excursion that does not exist in the organic carbon-isotopes. In Toka, the amplitude of the negative CIE is ~−4‰ in $\delta^{13}\text{C}_{\text{carb}}$ and ~−7‰ in $\delta^{13}\text{C}_{\text{org}}$. The inequality in amplitude of the excursions in carbonate and organic matter is a phenomenon seen in many but not all Toarcian sections (Hermoso et al., 2009; Jenkyns, 2010) and has been attributed to different fractionation effects of biological components, changes in atmospheric content of CO_2 , seawater composition and diagenesis. It is notable that in the Toka section the amplitude of the negative CIE is similar to that at Kastelli, in the Pindos Zone of Greece (Kafousia et al., 2011), Valdoria, Italy (Sabatino et al., 2009), Peniche, Portugal (Hesselbo et al., 2007) as well as in other European sections (Fig. 8).

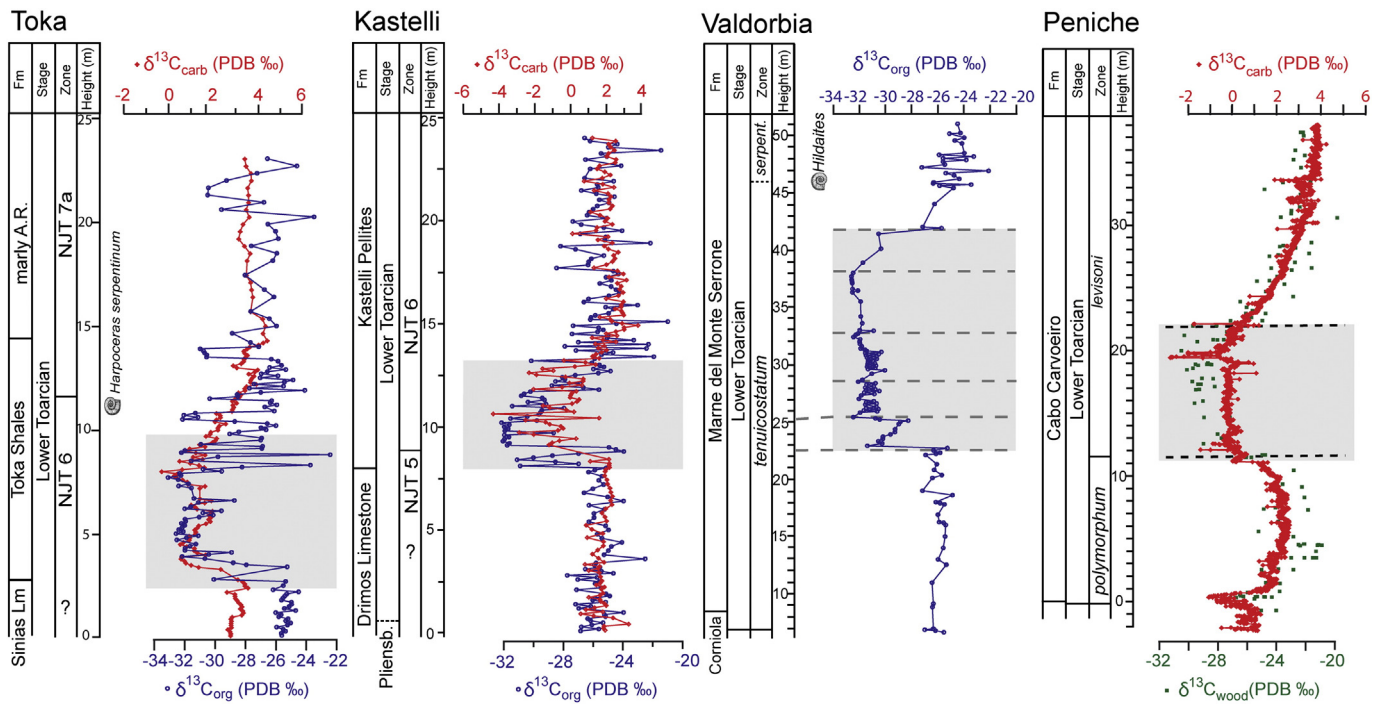


Fig. 8. Comparison of $\delta^{13}\text{C}_{\text{carb}}$ and $\delta^{13}\text{C}_{\text{org}}$ profiles from Toka section, with $\delta^{13}\text{C}_{\text{carb}}$ and $\delta^{13}\text{C}_{\text{org}}$ profiles from Kastelli section, Greece (Kafousia et al., 2011), $\delta^{13}\text{C}_{\text{org}}$ profile from Valdorbia, Italy (Sabatino et al., 2009), and $\delta^{13}\text{C}_{\text{carb}}$ and $\delta^{13}\text{C}_{\text{wood}}$ profile from Peniche, Portugal (Hesselbo et al., 2007). The shaded area marks the negative CIE.

Additionally, the Petousi section presents a positive CIE in both carbon isotopes from the 6 metre level of the section and onwards. The negative CIE of 1‰ in $\delta^{13}\text{C}_{\text{carb}}$ and of 5‰ in $\delta^{13}\text{C}_{\text{org}}$ in this section spans an interval of only ~2 m, but there follows a positive excursion of 1‰ for 11 metres in $\delta^{13}\text{C}_{\text{carb}}$ and of 4‰ for ~4 m in $\delta^{13}\text{C}_{\text{org}}$. The CIEs in both carbon-isotope curves look very similar to those in the shallow-water platform-carbonate section from Monte Sorgenza in southern Italy and Croatia (Trecalli et al., 2012; Sabatino et al., 2013), as can be seen in Fig. 9.

5.5. Temperature trend

Although oxygen-isotope ratios provide information on the palaeotemperature of precipitation or secretion of calcium carbonate, all lithified limestones carry some degree of diagenetic overprint. In the case of the Ionian sections, because of the poor preservation of the nannofossils that are mostly overgrown, the isotopes probably only reveal the overall temperature trend. The $\delta^{18}\text{O}_{\text{carb}}$ in all sections fluctuates between −4 and 0‰, which represent typical Toarcian

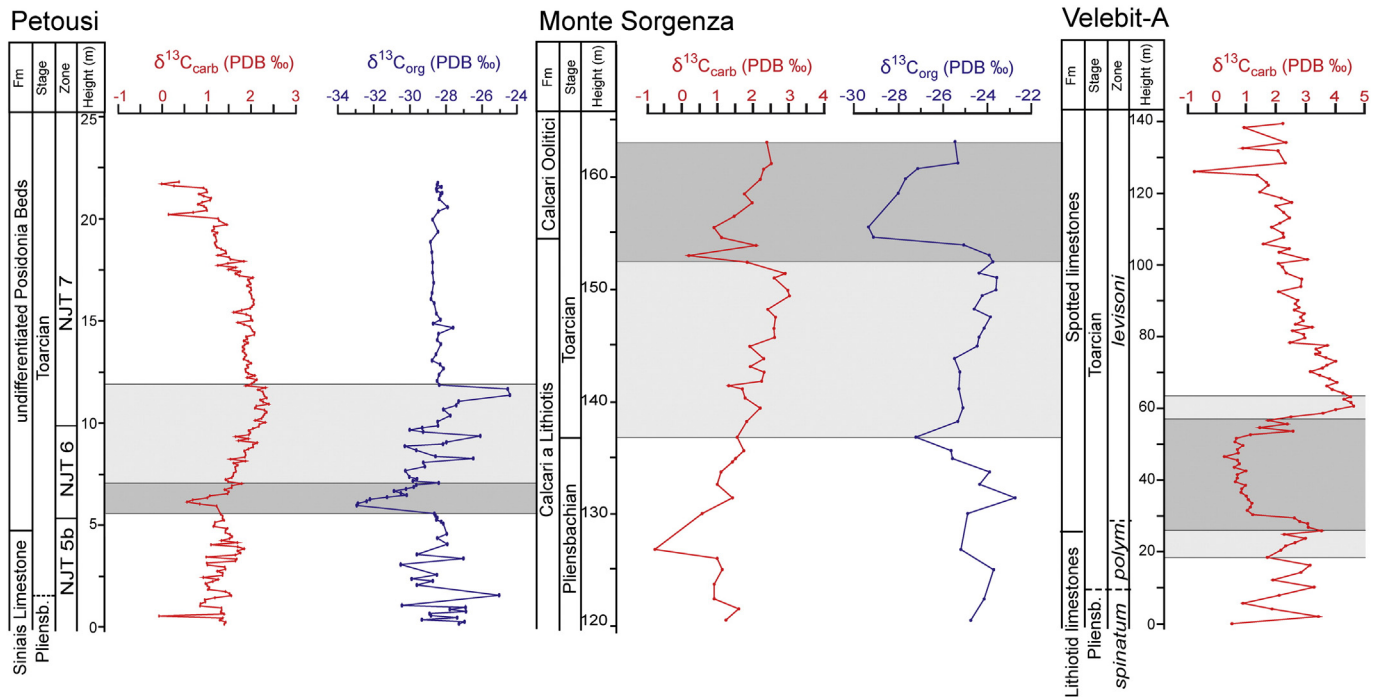


Fig. 9. Comparison of $\delta^{13}\text{C}_{\text{carb}}$ and $\delta^{13}\text{C}_{\text{org}}$ profiles from Petousi, $\delta^{13}\text{C}_{\text{carb}}$ and $\delta^{13}\text{C}_{\text{org}}$ profiles from Monte Sorgenzza, Italy (Trecalli et al., 2012) and $\delta^{13}\text{C}_{\text{carb}}$ profile from Velebit-A, Croatia (Sabatino et al., 2013). The deep grey colour shaded area represents the main negative CIE, while the light grey the positive excursions as there has been recorded in each section.

values (Jenkyns and Clayton, 1986; Bailey et al., 2003; Rosales et al., 2004; van de Schootbrugge et al., 2005b; Metodiev and Koleva-Rekalova, 2008). In the Toka section, a potential cooler event preceding a warm event coincides with the positive TOC excursion, a relationship also seen in other European sections (Bailey et al., 2003; Rosales et al., 2004; van de Schootbrugge et al., 2005b; Suan et al., 2010; Kafousia et al., 2011; Dera and Donnadieu, 2012; Harazim et al., 2012). These observations, coupled with the medium Pearson correlation coefficient r between carbon- and oxygen-isotope values (Supplementary data, S4), suggest that the diagenetic overprint was relatively modest and that the $\delta^{18}\text{O}_{\text{carb}}$ trends record genuine palaeotemperature variation.

6. Conclusions

Two high- and one low-resolution isotope records from the pelagic Toarcian sediments of the Ionian Zone have yielded new chemostratigraphic and biostratigraphic data. The Petousi section in the Ionian Zone records the Pliensbachian–Toarcian boundary in the upper metres of the Siniás Limestone, which belongs to Nannofossil Zone NJT 5. The stratigraphically higher formation (Toka Shales, undifferentiated Posidonia Beds or lower Posidonia Beds) is of Lower Toarcian Stage and belongs to Nannofossil Zone NJT 6. This Zone corresponds to the negative CIE and the positive excursion in TOC. The positive excursion, which is evident in both carbonate and organic carbon-isotopes in Petousi section, and also in the carbonate carbon-isotopes from Toka, occurs in Nannofossil Zone NJT 7.

The minor differences in lithology of the studied sections are interpreted as due to their belonging to different sub-basins of the Ionian Zone. Local environmental controls have likely governed the geochemical records of each locality. The TOC values are quite high in the two high-resolution datasets (Toka and Petousi: values up to 5 wt.%), similar to other sections from Tethyan Europe. However, in the Petousi section, values do not return to background levels following the excursion, as they do in Toka, but fluctuate up to the top of the section between 0 and 3 wt.%. In the Chionistra section, sampled at low-resolution, TOC values do not exceed 2 wt.%.

The high-resolution $\delta^{13}\text{C}$ curves of Toka and Petousi differ slightly in terms of not only trends but also of absolute $d^{13}\text{C}$ values. The Toka section records a small positive excursion only in carbonate carbon isotopes, whereas the Petousi section records a positive excursion in both carbon isotopes. The Toka section carbon-isotope profile has similarities with Kastelli, Pindos Zone, Greece (Kafousia et al., 2011), Peniche, Portugal (Hesselbo et al., 2007), Sancerre, Paris Basin (Hermoso et al., 2012), and other European sections, whereas the profile from Petousi is similar only to that from the shallow-water carbonates of Monte Sorgenza, southern Italy (Trecalli et al., 2012) and Velebit-A, Croatia (Sabatino et al., 2013).

The temperature trend in all the three sections is similar and records a cooler interval before the main warm event of the Early Toarcian: a pattern seen in many European sections.

All the data indicate that the Toarcian Oceanic Anoxic Event, characterized by deposition of organic-rich deposits, affected the sedimentation and the chemistry of seawater in the Ionian Zone. Slight variations in isotopic signature and pattern of organic-carbon enrichments indicate local variation on a global palaeoceanographic pattern.

Supplementary data to this article can be found online at <http://dx.doi.org/10.1016/j.palaeo.2013.11.013>.

Acknowledgements

The authors would like to thank Lutomir Metodiev (Bulgarian Academy of Science) for the identification of the ammonite. We would also like to thank Norman Charnley (Earth Sciences Department) and Peter Ditchfield (Archaeological Research Laboratory) for isotope analyses performed during a visit of NK to Oxford University. NK acknowledges the European Association of Organic Geochemists

(EAOG) for the travel scholarship that she received; and the University of Athens SARG for co-funding the field work.

References

- Al-Suwaidi, A.H., Angelozzi, G.N., Baudin, F., Damborenea, S.E., Hesselbo, S.P., Jenkyns, H.C., Manceñido, M.O., Riccardi, A.C., 2010. First record of the Early Toarcian Oceanic Anoxic Event from the Southern Hemisphere, Neuquén Basin, Argentina. *J. Geol. Soc.* 167, 633–636.
- Aubouin, J., 1959. Contribution à l'étude géologique de la Grèce septentrionale: les confins de l'Epire et de la Thessalie. *Ann. Géol. Pays Hellén.* 1, 1–483.
- Bailey, T.R., Rosenthal, Y., McArthur, J.M., van der Schootbrugge, B., 2003. Paleoceangoanographic changes of the Late Pliensbachian–Early Toarcian interval: a possible link to the genesis of an Oceanic Anoxic Event. *Earth Planet. Sci. Lett.* 212, 307–320.
- Baudin, F., Herbin, J.P., Bassoulet, J.P., Dercourt, J., Lachkar, G., Manivit, H., Renard, M., 1990. Distribution of organic matter during the Toarcian in the Mediterranean Tethys and Middle East. In: Huc, A.Y. (Ed.), *Deposition of Organic Facies*. American Association of Petroleum Geologists, *Studies in Geology*, 30, pp. 73–92.
- Bellanca, A., Masetti, D., Neri, R., Venezia, F., 1999. Geochemical and sedimentological evidence of productivity cycles recorded in Toarcian Black Shales from the Belluno Basin, Southern Alps, Northern Italy. *J. Sediment. Res.* 69, 466–476.
- Bernoulli, D., Renz, O., 1970. Jurassic carbonate facies and new ammonite faunas from Western Greece. *Eoclogae Geol. Helv.* 63, 573–607.
- Bodin, S., Mattioli, E., Fröhlich, S., Marshall, J.D., Boutib, L., Lahsini, S., Redfern, J., 2010. Toarcian carbon isotope shifts and nutrient changes from the Northern margin of Gondwana (High Atlas, Morocco, Jurassic): palaeoenvironmental implications. *Palaeogeogr. Palaeoclimatol. Palaeoecol.* 297, 377–390.
- Bown, P.R., Young, J., 1998. Chapter 2: techniques. In: Bown, P.R. (Ed.), *Calcareous Nannofossil Biostratigraphy*. Kluwer Academic Publishing, Dordrecht, pp. 16–28.
- Caruthers, A.H., Gröcke, D.R., Smith, P.L., 2011. The significance of an Early Jurassic (Toarcian) carbon-isotope excursion in Haida Gwaii (Queen Charlotte Islands), British Columbia, Canada. *Earth Planet. Sci. Lett.* 307, 19–26.
- Dera, G., Donnadieu, Y., 2012. Modeling evidences for global warming, Arctic seawater freshening, and sluggish oceanic circulation during the Early Toarcian Anoxic Event. *Paleoceanography* 27, PA2211. <http://dx.doi.org/10.1029/2012PA002283>.
- Dera, G., Neige, P., Dommergues, J.-L., Brayard, A., 2011. Ammonite paleobiogeography during the Pliensbachian–Toarcian crisis (Early Jurassic) reflecting paleoclimate, eustasy, and extinctions. *Glob. Planet. Chang.* 78, 92–105.
- Dommergues, J.-L., Karakitsios, V., Meister, C., Bonneau, M., 2002. New ammonite data about the earliest syn-rift deposits (Lower Jurassic) in the Ionian Zone of N-W Greece (Epirus). *N. Jb. Geol. Paläont. (Abh.)* 223, 299–316.
- Gill, B.C., Lyons, T.W., Jenkyns, H.C., 2011. A global perturbation to the sulfur cycle during the Toarcian Oceanic Anoxic Event. *Earth Planet. Sci. Lett.* 312, 484–496.
- Gröcke, D.R., Hori, R.S., Trabucho-Alexandre, J., Kemp, D.B., Schwark, L., 2011. An open ocean record of the Toarcian Oceanic Anoxic Event. *Solid Earth* 2, 245–257.
- Harazim, D., van de Schootbrugge, B.A.S., Sorichter, K., Fiebig, J., Weug, A., Suan, G., Oschmann, W., 2012. Spatial variability of watermass conditions within the European Epicontinental Seaway during the Early Jurassic (Pliensbachian–Toarcian). *Sedimentology* 60, 359–390. <http://dx.doi.org/10.1111/j.1365-3091.2012.01344.x>.
- Hermoso, M., Le Callonnec, L., Minoletti, F., Renard, M., Hesselbo, S.P., 2009. Expression of the Early Toarcian negative carbon-isotope excursion in separated carbonate microfractions (Jurassic, Paris Basin). *Earth Planet. Sci. Lett.* 277, 194–203.
- Hermoso, M., Minoletti, F., Rickaby, R.E.M., Hesselbo, S.P., Baudin, F., Jenkyns, H.C., 2012. Dynamics of a stepped carbon-isotope excursion: Ultra high-resolution study of Early Toarcian environmental change. *Earth Planet. Sci. Lett.* 319–320, 45–54.
- Hesselbo, S.P., Gröcke, D.R., Jenkyns, H.C., Bjerrum, C.J., Farrimond, P., Morgans Bell, H.S., Green, O.R., 2000. Massive dissociation of gas hydrate during a Jurassic oceanic anoxic event. *Nature* 406, 392–395.
- Hesselbo, S.P., Jenkyns, H.C., Duarte, L.V., Oliveira, L.C.V., 2007. Carbon-isotope record of the Early Jurassic (Toarcian) Oceanic Anoxic Event from fossil wood and marine carbonates (Lusitanian Basin, Portugal). *Earth Planet. Sci. Lett.* 253, 455–470.
- Hönisch, B., Ridgwell, A., Schmidt, D.N., Thomas, E., Gibbs, S.J., Sluijs, A., Zeebe, R., Kump, L., Martindale, R.C., Greene, S.E., Kiessling, W., Ries, J., Zachos, J.C., Royer, D.L., Barker, S., Marchitto, T.M., Moyer, R., Pelejero, C., Ziveri, P., Foster, G.L., Williams, B., 2012. The geological record of ocean acidification. *Science* 335, 1058–1063.
- IGRS-IFP (Institut de Géologie et Recherches du Sous-Sol, Athènes, et Institut français du Pétrole, Mission Grèce), 1966. *Étude Géologique de l'Epire (Grèce Nord-Occidentale)*. Editions Technip, Paris (306 pp.).
- Jenkyns, C.H., 1985. The Early Toarcian and Cenomanian–Turonian anoxic events in Europe: comparisons and contrasts. *Geol. Rundsch.* 74, 505–518.
- Jenkyns, H.C., 1988. The Early Toarcian (Jurassic) anoxic event: stratigraphic, sedimentary, and geochemical evidence. *Am. J. Sci.* 288, 101–151.
- Jenkyns, H.C., 2003. Evidence for rapid climate change in the Mesozoic–Palaeogene greenhouse world. *Philos. Trans. R. Soc. Lond. Ser. A* 361, 1885–1916.
- Jenkyns, H.C., 2010. Geochemistry of oceanic anoxic events. *Geochem. Geophys. Geosyst.* 11. <http://dx.doi.org/10.1029/2009GC002788>.
- Jenkyns, H.C., Clayton, C.J., 1986. Black shales and carbon isotopes in pelagic sediments from the Tethyan Lower Jurassic. *Sedimentology* 33, 87–106. <http://dx.doi.org/10.1111/j.1365-3091.1986.tb00746.x>.
- Jenkyns, H., Clayton, C., 1997. Lower Jurassic epicontinental carbonates and mudstones from England and Wales: chemostratigraphic signals and the Early Toarcian Anoxic Event. *Sedimentology* 44, 687–706. <http://dx.doi.org/10.1046/j.1365-3091.1997.d01-43.x>.

- Jenkyns, H.C., Gale, A.S., Corfield, R.M., 1994. Carbon- and oxygen-isotope stratigraphy of the English Chalk and Italian Scaglia and its palaeoclimatic significance. *Geol. Mag.* 131, 1–34.
- Jenkyns, H.C., Gröcke, D.R., Hesselbo, S.P., 2001. Nitrogen-isotope evidence for watermass denitrification during the Early Toarcian (Jurassic) Oceanic Anoxic Event. *Paleoceanography* 16, 593–603. <http://dx.doi.org/10.1029/2000PA000558>.
- Jenkyns, H.C., Matthews, A., Tsikos, H., Erel, Y., 2007. Nitrate reduction, sulfate reduction, and sedimentary iron isotope evolution during the Cenomanian–Turonian oceanic anoxic event. *Paleoceanography* 22, PA3208. <http://dx.doi.org/10.1029/2006PA001355>.
- Kafousia, N., Karakitsios, V., Jenkyns, H.C., Mattioli, E., 2011. A global event with a regional character: the Early Toarcian Oceanic Anoxic Event in the Pindos Ocean (Northern Peloponnese, Greece). *Geol. Mag.* 148, 619–631.
- Karakitsios, V., 1992. Ouverture et inversion tectonique du bassin Ionien (Epire, Grèce). *Ann. Géol. Pays Hellén.* 35, 185–318.
- Karakitsios, V., 1995. The influence of preexisting structure and halokinesis on organic matter preservations and thrust system evolution in the Ionian basin, Northwest Greece. *Am. Assoc. Pet. Geol. Bull.* 79, 960–980.
- Karakitsios, V., Rigakis, N., 2007. Evolution and petroleum potential of Western Greece. *J. Pet. Geol.* 30, 197–218.
- Karakitsios, V., Tsaila-Monopolis, S., 1988. Données nouvelles sur les niveaux supérieurs (Lias inférieur-moyen) des Calcaires de Pantokrator (zone Ionienne moyenne, Epire, Grèce continentale). Description des Calcaires de Louros. *Rev. Micropaléontologie* 31, 49–55.
- Karakitsios, V., Velitzelos, E., 1994. Discovery of the conifer *Brachyphyllum nepos* SAPORTA in the Lower Posidonia Beds (Toarcian) of the Ionian Zone (Epirus, NW-Greece). *Bull. Geol. Soc. Greece* 30/2, 207–215 (in Greek).
- Karakitsios, V., Danielian, T., De Wever, P., 1988. Datations par les Radiolaires à Filaments, Schistes à Posidonia superieurs et Calcaires de Vigla (zone Ionienne, Epire, Grèce) du Callovien au Tithonique terminal. *C. R. Acad. Sci. Paris* 306, 367–372.
- Karakitsios, V., Kafousia, N., Tsikos, H., 2010. A review of oceanic anoxic events as recorded in the Mesozoic sedimentary record of mainland Greece. *Hell. J. Geosci.* 45, 123–132.
- Laubscher, H., Bernoulli, D., 1977. Mediterranean and Tethys. In: Biju-Duval, Bernard, Montadert, Lucien (Eds.), *Structural History of the Mediterranean Basins*. Éditions Technip, pp. 129–132.
- Léonide, P., Floquet, M., Durlet, C., Baudin, F., Pittet, B., Lécuyer, C., 2012. Drowning of a carbonate platform as a precursor stage of the Early Toarcian global anoxic event (Southern Provence sub-Basin, South-east France). *Sedimentology* 59, 156–184. <http://dx.doi.org/10.1111/j.1365-3091.2010.01221.x>.
- Little, C.T.S., Benton, M.J., 1995. Early Jurassic mass extinction: a global long-term event. *Geology* 23, 495–498.
- Littler, K., Hesselbo, P.S., Jenkyns, H.C., 2010. A carbon-isotope perturbation at the Pliensbachian–Toarcian boundary: evidence from the Lias Group, NE England. *Geol. Mag.* 147, 181–192.
- Mailliot, S., Mattioli, E., Bartolini, A., Baudin, F., Pittet, B., Guex, J., 2009. Late Pliensbachian–Early Toarcian (Early Jurassic) environmental changes in an epicontinental basin of NW Europe (Causse area, central France): a micropaleontological and geochemical approach. *Palaeogeogr. Palaeoclimatol. Palaeoecol.* 273, 346–364.
- Mattioli, E., Erba, E., 1999. Synthesis of calcareous nannofossil events in Tethyan Lower and Middle Jurassic successions. *Riv. Ital. Paleontol. Stratigr.* 105, 343–376.
- Mattioli, E., Pittet, B., Bucefalo Palliani, R., Röhrl, H.-J., Schmid-Röhrl, A., Morettini, E., 2004. Phytoplankton evidence for the timing and correlation of palaeoceanographical changes during the early Toarcian Oceanic Anoxic Event (Early Jurassic). *J. Geol. Soc. Lond.* 161, 685–693.
- Mattioli, E., Pittet, B., Petitpierre, L., Mailliot, S., 2009. Dramatic decrease of pelagic carbonate production by nannoplankton across the Early Toarcian Anoxic Event (T-OAE). *Glob. Planet. Chang.* 65, 134–145.
- Mazzini, A., Svensen, H., Leanza, H.A., Corfu, F., Planke, S., 2010. Early Jurassic shale chronostratigraphy and U-Pb ages from the Neuquén Basin (Argentina): implications for the Toarcian Oceanic Anoxic Event. *Earth Planet. Sci. Lett.* 297, 633–645.
- Metodiev, L., 2008. The Ammonite Zones of the Toarcian in Bulgaria – new evidence, subzonation and correlation with the standard Zones and subzones in north-western Europe. *C. R. Acad. Bulg. Sci.* 61, 87–132.
- Metodiev, L., Koleva-Rekalova, E., 2008. Stable isotope records ($\delta^{18}\text{O}$) and ($\delta^{13}\text{C}$) of Lower-Middle Jurassic belemnites from the Western Balkan mountains (Bulgaria): palaeoenvironmental application. *Appl. Geochem.* 23, 2845–2856.
- Newton, R.J., Reeves, E.P., Kafousia, N., Wignall, P.B., Bottrell, S.H., Sha, J.-G., 2011. Low marine sulfate concentrations and the isolation of the European epicontinental sea during the Early Jurassic. *Geology* 39, 7–10.
- Pancost, R.D., Crawford, N., Magness, S., Turner, A., Jenkyns, H.C., Maxwell, J.R., 2004. Further evidence for the development of photic-zone euxinic conditions during Mesozoic oceanic anoxic events. *J. Geol. Soc. Lond.* 161, 353–364.
- Renz, C., 1910. Die Geologie Griechenlands. I. Teil. Stratigraphische Untersuchungen im griechischen Mesozoikum und Paläozoikum. *Jb. K.-Kg. Geol. Reichsanst. Wien* 60, 421–636.
- Rigakis, N., Karakitsios, V., 1998. The source rock horizons of the Ionian Basin (NW Greece). *Mar. Pet. Geol.* 15, 593–617.
- Rosales, I., Robles, S., Quesada, S., 2004. Elemental and oxygen isotope composition of Early Jurassic belemnites; salinity vs. temperature signals. *J. Sediment. Res.* 74, 342–354.
- Sabatino, N., Neri, R., Bellanca, A., Jenkyns, H.C., Baudin, F., Parisi, G., Masetti, D., 2009. Carbon-isotope records of the Early Jurassic (Toarcian) oceanic anoxic event from the Valdorbia (Umbria–Marche Apennines) and Monte Mangart (Julian Alps) sections: paleoceanographic and stratigraphic implications. *Sedimentology* 56, 1307–1328. <http://dx.doi.org/10.1111/j.1365-3091.2008.01035.x>.
- Sabatino, N., Neri, R., Bellanca, A., Jenkyns, H.C., Masetti, D., Scopelliti, G., 2011. Petrography and high-resolution geochemical records of Lower Jurassic manganese-rich deposits from Monte Mangart, Julian Alps. *Palaeogeogr. Palaeoclimatol. Palaeoecol.* 299, 97–109.
- Sabatino, N., Vlahović, I., Jenkyns, H.C., Scopelliti, G., Neri, R., Prtoljan, B., Velić, I., 2013. Carbon-isotope record and palaeoenvironmental changes during the early Toarcian oceanic anoxic event in shallow-marine carbonates of the Adriatic carbonate platform in Croatia. *Geol. Mag.* 150, 1085–1102.
- Sælen, G., Doyle, P., Talbot, M.R., 1996. Stable-isotope analyses of Belemnite Rostra from the Whitby Mudstone Fm., England: surface water conditions during deposition of a marina black shale. *PALAIOS* 11, 97–117.
- Suan, G., Mattioli, E., Pittet, B., Mailliot, S., Lécuyer, C., 2008. Evidence for major environmental perturbation prior to and during the Toarcian (Early Jurassic) oceanic anoxic event from the Lusitanian Basin, Portugal. *Paleoceanography* 23, PA1202. <http://dx.doi.org/10.1029/2007PA001459>.
- Suan, G., Mattioli, E., Pittet, B., Lécuyer, C., Suchuras-Marx, B., Duarte, L.V., Philippe, M., Reggiani, L., Martineau, F., 2010. Secular environmental precursors to Early Toarcian (Jurassic) extreme climate changes. *Earth Planet. Sci. Lett.* 290, 448–458.
- Suan, G., Nikitenko, B.L., Rogov, M.A., Baudin, F., Spangenberg, J.E., Knyazev, V.G., Glinskikh, L.A., Goryacheva, A.A., Adatte, T., Riding, J.B., Föllmi, K.B., Pittet, B., Mattioli, E., Lécuyer, C., 2011. Polar record of Early Jurassic massive carbon injection. *Earth Planet. Sci. Lett.* 312, 102–113.
- Svensen, H., Planke, S., Chevallier, L., Malthe-Sorensen, A., Corfu, F., Jamtveit, B., 2007. Hydrothermal venting of greenhouse gases triggering Early Jurassic global warming. *Earth Planet. Sci. Lett.* 256, 554.
- Trecalli, A., Spangenberg, J., Adatte, T., Föllmi, K.B., Parente, M., 2012. Carbonate platform evidence of ocean acidification at the onset of the Early Toarcian Oceanic Anoxic Event. *Earth Planet. Sci. Lett.* 357–358, 214–225.
- van Breugel, Y., Baas, M., Schouten, S., Mattioli, E., Sinninghe Damsté, J.S., 2006. Isorenieratane record in black shales from the Paris Basin, France: constraints on recycling of residual CO_2 as a mechanism for negative carbon isotope shifts during the Toarcian Oceanic Anoxic Event. *Paleoceanography* 21, PA4220. <http://dx.doi.org/10.1029/2006PA001305>.
- van de Schootbrugge, B., Bailey, T.R., Rosenthal, Y., Katz, M.E., Wright, J.D., Miller, K.G., Feist-Burkhardt, S., Falkowski, P.G., 2005a. Early Jurassic climate change and the radiation of organic-walled phytoplankton in the Tethys Ocean. *Paleobiology* 31, 73–97.
- van de Schootbrugge, B., McArthur, J.M., Bailey, T.R., Rosenthal, Y., Wright, J.D., Miller, K.G., 2005b. Toarcian oceanic anoxic event: an assessment of global causes using belemnite C isotope records. *Paleoceanography* 20, PA3008. <http://dx.doi.org/10.1029/2004PA001102>.
- Walzebuck, J.P., 1982. Bedding types of the Toarcian black shales in NW Greece. In: Einsele, G., Seilacher, A. (Eds.), *Cyclic and Event Stratification*. Springer, Berlin, pp. 512–525.
- Wignall, P.B., 2001. Large igneous provinces and mass extinctions. *Earth Sci. Rev.* 53, 1–33.
- Woodfine, R.G., Jenkyns, H.C., Sarti, M., Baroncini, F., Violante, C., 2008. The response of two Tethyan carbonate platforms to the early Toarcian (Jurassic) Oceanic Anoxic Event: environmental change and differential subsidence. *Sedimentology* 55, 1011–1028. <http://dx.doi.org/10.1111/j.1365-3091.2007.00934.x>.